Extension of the lattice-based aggregation-volume-bias Monte

Carlo approach to molecular crystals: Quantitative calculations on

the thermodynamic stability of the urea polymorphs

Bin Chen*

Department of Chemistry, Louisiana State University, Baton Rouge, Louisiana 70803-1804,

USA

ABSTRACT

Motivated by the recent success in using a latticed-based version of the aggregation-volume-bias

Monte Carlo method to determine the thermodynamic stabilities of both bcc and fcc clusters

formed by Lennard-Jones particles, this approach is extended to the calculation of the nucleation

free energies of solid clusters formed by urea at 300 K in two different polymorphs, i.e., form I

and form IV. In addition to the lattice confinement, constraint on the molecular orientation was

found necessary to ensure that the clusters sampled in these simulations are in the corresponding

form. A model that can reproduce the experimental properties such as density and lattice

parameters of form I at ambient conditions is used in this study. From the size dependencies of the

free energies obtained for a finite set of clusters studied, the free energies of clusters at other sizes

including an infinitely large cluster were extrapolated. At the infinite size, equivalent to a bulk

solid, form I was found to be more stable than form IV, which agrees with the experimental results.

In addition, form I was found to be thermodynamically stable throughout the entire cluster size

range investigated here, contrary to the previous finding that small form I clusters are unstable

from the crystal nucleation simulation studies.

*Corresponding author: email: binchen@lsu.edu

1

I. INTRODUCTION

Since the seminal work in 1953 by Metropolis et al., the Monte Carlo method has been known for its flexibility to incorporate unphysical moves to sample the phase space of complex fluid, which is in stark contrast to the natural time evolution used by molecular dynamics. Due to this flexibility, advanced and efficient schemes that explore the use of unphysical moves can be developed to accelerate the phase space sampling and to bridge the time scales of the real events. One example is the aggregation-volume-bias Monte Carlo (AVBMC) method^{2,3} where goaloriented moves are used to efficiently sample clusters of different sizes for a faster convergence of their free energies critical to the understanding of the long time-scale nucleation events encountered in phase transition, such as vapor to liquid nucleation.⁴⁻⁶ In a recent development,⁷ this approach is extended to solid systems where a new type of AVBMC moves is introduced to bring particles directly to a region near the lattice site to avoid the formation of liquid-like clusters that are otherwise encountered when using the regular AVBMC. Further, the lattice sites can be arranged in any specific polymorphic form so that the free energies of clusters with different solid structures can be calculated.⁸ These free energy results obtained at finite number of cluster sizes can be used to formulate a thermodynamic relation, which allows for the prediction of the free energies of clusters at other sizes including an infinitely large cluster (equivalent to a bulk phase). As a result, the entire thermodynamic landscape (i.e., free energies for clusters of different structures and sizes, including an infinitely large cluster or the bulk phase) can be revealed, which is critical to the understanding of the formation of polymorphs.

Motivated by the recent success in using a latticed-based version of the aggregation-volume-bias Monte Carlo (LB-AVBMC) method to determine the thermodynamic stabilities of both bcc and fcc clusters formed by Lennard-Jones particles, ^{7,8} this approach is extended to the calculation

of the nucleation free energies of solid clusters formed by urea. Urea has been known experimentally to exist in many polymorphic forms, including forms I, III, IV, and V.9-12 In a recent computational work, 13 nine selected GAFF14 (Generalized AMBER15 Force Field) and OPLS¹⁶ (Optimized Potential for Liquid Simulations) force fields were examined in terms of how well they can reproduce the experimental properties of these forms. It was shown that all force fields overestimated the density by 6% or more compared to the experimental density for form I which is known to be most stable in ambient conditions. Some of the force fields clearly fail to reproduce the thermodynamic stabilities of these forms as simulations starting with the most stable crystal form, i.e., form I, ended at a different structure. For the rest that retain the most stable crystal form, it is unclear that they can indeed predict the experimental thermodynamic stabilities of these forms as simulations starting with form IV, known experimentally to be less stable, stayed at that form as well throughout the entire simulation. Determination of the thermodynamic stabilities of polymorphs requires the free energy information, which is a challenging problem for solids. For this part, the Einstein crystal method¹⁷⁻¹⁹ remains to be the dominant approach which has been applied to a few molecular systems such as water and methanol²⁰ but not urea. In addition, the few crystal nucleation related theoretical studies on urea²¹⁻²³ all suggest an interesting crossover of the thermodynamic stability from one form to another during the early stage of this process, reminiscent of the crossover from bcc to fcc observed in the LJ system.^{8,24} It makes one wonder, is this crossover a common behavior in crystallization? The ability to calculate free energies for both clusters and bulk phases of different forms makes the AVBMC approach ideal for this investigation.

II. METHODS

The model used in this study was based on an improved GAFF, specifically GAFF-D3,²⁵ as it was found to be one of the best overall performing force fields in terms of predicting the properties in both the crystal and the solution phases. 13 Most of the intramolecular parameters and all partial charges are borrowed from this force field, whereas the van der Waals parameters are from TraPPE (Transferable Potentials for Phase Equilibria)²⁶ combined with the Lorentz-Berthelot^{27,28} mixing rules. It is a fully rigid model with both bond lengths and angles fixed. Listed in Table 1 are the parameters of this model. This modified model was found to reproduce well the experimental density of the most stable form (i.e., form I) in ambient conditions. For example, at 300 K and 1 atm, it yields a density of 1.307±0.001 g/cm³ compared to the experimental density of 1.33 g/cm³.²⁹ In contrast, the original GAFF-D3 force field predicted a density around 1.459±0.006 g/cm³.13 This modified model yields the following lattice parameters: $a = 5.625 \pm 0.004$ Å, $b = 5.625 \pm 0.004$ Å, and $c = 4.819 \pm 0.001$ Å, compared to $a = b = 5.662 \pm 0.002$ Å and $c = 4.716 \pm 0.002$ Å from the experiment, 30 vs. $a = 5.398 \pm 0.082$ Å, $b = 5.400 \pm 0.082$ Å, $c = 4.691 \pm 0.011$ Å by GAFF-D3. 13 The cohesive energy predicted by this model is -92.8±0.1 kJ/mol, compared to -91.9±0.4 kJ/mol by GAFF-D3.¹³ The experimental value ranges from -87.65 to -98.58 kJ/mol. ³¹⁻³⁵ All these results were obtained from NPT simulations using 432 particles (or 6 × 6 × 6 supercell). Spherical potential truncation at 14 Å were used for both the LJ and the real-space part of the Coulombic interactions. While an analytical tail correction was used for the LJ interactions, an Ewald sum³⁶ with a kappa value of 0.23 Å⁻¹ and tin-foil boundary conditions were used to treat the long-range electrostatic interactions.

Four different crystal structures have been discovered by the experiments, i.e., forms I, III, IV, and V, with lattice parameters only available for the first three. The results presented above

from NPT simulations are for form I, the most stable form at ambient conditions whereas the other forms exist at high pressure conditions for the real system. According to the simulation results obtained by Anker et al., ¹³ form IV, although shown by the experiments as a high-pressure form, may have a thermodynamic stability close to that of form I as for some of the force fields simulations starting with a form I structure show a conversion to a form IV or a distorted I/IV structure. In addition, form IV resembles the other form found to be more stable than form I but was named as form II (or 2) by the previous crystal nucleation studies (see Figure 1). Thus, both form I and form IV are included in this study. Additional NPT simulations at 300 K and 1 atm were performed for form IV using an $8 \times 4 \times 7$ supercell, which yielded the following lattice parameters: $a = 4.024 \pm 0.002 \text{ Å}$, $b = 7.666 \pm 0.004 \text{ Å}$, $c = 4.706 \pm 0.002 \text{ Å}$. These lattice parameters combined with the relative positions of the carbon atoms were used to construct the lattice needed for the LB-AVBMC simulations. Specifically, the AVBMC moves, which allow particles to be transferred from one phase to another, are directed toward a region near one of the lattice positions adjacent to a target particle selected from the cluster. This method is naturally suited for solid systems as each particle oscillates around its lattice position within its own volume (see Fig. 2). In the case of urea, the carbon atom needs to be within a certain radius, r, away from the lattice position. This radius must be smaller than half of the distance between the closest pair of lattice sites since only one particle is allowed in each spherical region centered around each lattice site. All simulations were performed using r = 2 Å. Additional simulations were performed using regular AVBMC where particle transfer occurs at a spherical region centered around the target particle selected from the cluster, with a larger radius R of 6 Å. The acceptance rate of these AVBMC moves can be improved by Rosenbluth sampling with the multiple insertion scheme commonly used in configurational-bias Monte Carlo³⁷⁻⁴⁷ and further optimized with a preferential selection of the target particle near the surface region. ^{48,49} Surface particles have higher energies than those in the interior and can be preferentially picked as the target particle using an energy-based function. The acceptance rate would need to be modified to satisfy the detailed balance condition (see Ref. 49). Since successful particle transfer occurs most likely at the surface, the acceptance rate does not change much with the increase of the cluster size, ~0.5% for the cluster size range between 200 and 800, with this preferential selection scheme. In contrast, when the target particle is picked randomly from the cluster, the acceptance rate decreases significantly with the increase of the cluster size as shown previously for the LJ system.⁷

For computational efficiency, simulations were performed sparsely over a large size range, e.g., for clusters containing 200±2, 400±2, and 800±2 particles. The grand canonical ensemble^{4,50,51} is used for all nucleation simulations whereas the cluster is physically isolated but thermodynamically connected to an ideal gas-phase at a certain chemical potential or density, ρ_v . While one third of Monte Carlo moves are spent on particle transfer using AVBMC or LB-AVBMC, the rest are equally divided between translation and rotation around the carbon atom. Simulations for solid clusters start with a perfect crystal structure of a rectangular shape that has about 20% more particles than each cluster size picked for this study, e.g., an $8 \times 8 \times 8$ supercell for form I clusters with a target size range of 800 by evaporating the excess particles using a simulation run at a relative low gas phase density condition. After a few iterative runs to obtain the biasing potentials needed by the umbrella sampling⁵² technique used by these simulations and also to equilibrate the system, the free energy results, analyzed in terms of $\delta \Delta G = \Delta G(n) - \Delta G(n)$ -4) with $\Delta G(n)$ referring to the nucleation free energy at the cluster size n, appear to fluctuate around a certain value from one run to another. A few production runs are then used to estimate both the average and the error on the free energy results. All interactions are included in these

cluster simulations. The total simulation length of the production runs has $O(10^{11})$ Monte Carlo moves.

III. RESULTS AND DISCUSSION

Compared to LJ, urea molecules not only translate but also rotate. When the original LB-AVBMC was used, the lattice confinement was found to be insufficient to ensure that the clusters sampled are in the right form. As shown in Figure 2, molecules sampled using the form IV lattice parameters orient differently from those in the bulk phase even for clusters containing 800 molecules. For example, they tend to adopt an orientation with the molecular plane parallel to (or with the normal of the plane perpendicular to) the *z*-axis, like those in form I (see panel a of Figure 2). This issue can be fixed by adding an orientational constraint, i.e., restricting ϕ to be within the range expected for the corresponding form, i.e., within 0.15 π from π or 2π for form IV, chosen based on the observation that the ϕ distributions of these two forms barely overlap with each other (see panel b of Figure 2). Due to the change of the probability of choosing a ϕ angle within a small range over the entire 2π range (or the change of the phase space volume for the rotational part of the partition function), the acceptance rate for the AVBMC swap moves would need to be modified accordingly. This constraint appears to be sufficient to help retain form IV in the expected orientation even for small clusters (see panels c and d of Figure 2).

Shown in Figure 3 are the $\delta\Delta G$ results plotted as function of $n^{2/3} - (n-4)^{2/3}$ obtained at T = 300 K and $\rho_{\rm v} = 4 \times 10^{-11}$ molecule/Å³. This plot has been used to examine the error of the classical nucleation theory (CNT)⁵³⁻⁵⁶ and to extrapolate the results at other cluster sizes including the infinite size which is equivalent to the bulk phase.^{7,8,57-63} CNT derives the free energy formation of a cluster using a simple spherical droplet model where it is assumed to behave as an infinitely

large bulk phase (either liquid or solid) on properties including density ρ , surface tension γ , and chemical potential μ , i.e., $\Delta G(n) = n\Delta \mu + n^{2/3} (36\pi/\rho^2)^{1/3} \gamma$. 57,58,61 The bulk and the surface term differs in terms of the dependency on n. In particular, the surface term is equal to γ times the surface area, which can be shown to be equal to $n^{2/3}(36\pi/\rho^2)^{1/3}$ for a perfect spherical droplet with a density value of ρ . Thus, a plot of $\delta\Delta G$ (= $\Delta G(n) - \Delta G(n-4)$) as function of $n^{2/3} - (n-4)^{2/3}$ would fall onto a linear line with a slope of $(36\pi/\rho^2)^{1/3}\gamma$, and an intercept of $4 \times \Delta\mu$ where $\Delta\mu$ refers to the chemical potential difference between the bulk phase and the ideal gas phase at ρ_v (= 4 × 10^{-11} molecule/Å³). For all three types of clusters studied here, the $\delta\Delta G$ results follow this linear behavior. This linear dependence allows for a convenient extrapolation of the free energy results for other sizes including the infinite size, equivalent to the bulk phase. Thus, the thermodynamic stability of different polymorphs can be examined. As shown in Figure 3, linear fits to the clusters size range between 200 and 800 yield an intercept of -18.8±0.2 for form I, -14.9±0.7 (or -16.6 ± 0.3) for form IV with (or without) the ϕ constraint, and -10.3 ± 0.1 for liquid. For the model examined in this study, form I is more stable than form IV at this ambient condition, which agrees with the experiments.

The relatively thermodynamic stability of these two forms can be also observed from the bulk-phase simulations or the cluster nucleation study employing the regular AVBMC approach, used to sample liquid clusters, i.e., the form IV structure can be converted to form I in both types of simulations. The use of periodic boundary conditions and a relatively small system in bulk phase simulations can retain the form IV structure within the simulation length (on the order of 10^4 Monte Carlo cycles) so that the lattice parameter can be obtained. However, all NPT simulations on a slightly larger $8 \times 5 \times 7$ supercell of the form IV structure and all cluster simulations using regular AVBMC end at a form I structure. Even those simulations using LB-AVBMC starting with a form

IV structure show tendency to evolve into a form I structure, as indicated by the angular distributions of Figure 2 and by the further analysis of the order parameter $q_6^{64,65}$ (see Figure 4). This is opposite to the finding of the conversion of form I to form IV for small clusters from the previous simulation studies, which could be due to the use of different models. As shown by Anker et al., the performance of nine models investigated there differ wildly in terms of predicting properties such as density, lattice parameters, and thermodynamic stability. For example, while simulations using GAFF1 with a form I structure show a conversion to form IV at 400 K, simulations using GAFF-D3 reveal that this phase change can occur in an opposite direction (see Tables 7 and 8 from Ref. 13). Thus, quantitative determinations of the thermodynamic stability of different polymorphs have become important to fully understand the origin of polymorphism.

IV. CONCLUSIONS

In conclusion, this work presented an approach that has can reveal the entire thermodynamic landscape involved in the formation of molecular crystals, i.e., free energies for clusters of different structures and sizes including the infinite size (or equivalently the bulk phase). It was based on the lattice-based aggregation-volume-bias Monte Carlo approach that has been shown to be successful for quantitative determination of the thermodynamic stability of BCC and FCC crystals formed by the Lennard-Jones systems. For molecular crystals, the original LB-AVBMC was found to be insufficient to ensure that the crystals stay in the form intended. For the case of urea, it was found necessary to place an additional constraint on the molecular orientation to prevent form IV from its tendency to transform into form I. Using the size dependency of the free energy results obtained at a limited number of clusters, the free energy for clusters at other sizes can be extrapolated. At

the infinite size, which is equivalent to the bulk phase, form I was found to be more stable than form IV, which agrees with the experiments. This work presents the first application of LB-AVBMC to a molecular crystal. The contradictory finding of the thermodynamic stabilities of form I and form IV solid clusters to previous crystal nucleation studies results from the use of different force fields. This may inspire future experimental and theoretical research to determine which form is thermodynamically stable for small solid clusters.

The author would like to acknowledge Ilja Siepmann to bring him to the world of Monte Carlo and the financial support from the National Science Foundation (Grant No. CHE-2413803). Computational resources for this work are provided by the Louisiana Optical Network (LONI) and Louisiana State High Powered Computing Center (LSU-HPC).

DATA AVAILABILITY

The data that support the findings of this study are available from the corresponding author upon reasonable request.

REFERENCES

- 1. N. Metropolis, A. W. Rosenbluth, M. N. Rosenbluth, A. H. Teller, and E. Teller, J. Chem. Phys. **21**, 1087 (1953).
- 2. B. Chen and J. I. Siepmann, J. Phys. Chem. B 104, 8725 (2000).
- 3. B. Chen and J. I. Siepmann, J. Phys. Chem. B **105**, 11275 (2001).
- 4. B. Chen, J. I. Siepmann, K. J. Oh, and M. L. Klein, J. Chem. Phys. 115, 10903 (2001).
- 5. S. M. Kathmann, G. K. Schenter, B. C. Garrett, B. Chen, and J. I. Siepmann, J. Phys. Chem. C 113, 10354 (2009).
- 6. K. E. Ogunronbi, A. Sepehri, B. Chen, and B. E. Wyslouzil, J. Chem. Phys. **148**, 144312 (2018).
- 7. B. Chen, J. Phys. Chem. A **126**, 5517 (2022).
- 8. B. Chen, J. Chem. Phys. **159**, 071102 (2023).

- 9. A. Olejniczak, K. Ostrowska, and A. Katrusiak, J. Phys. Chem. C 113, 15761–15767 (2009).
- 10. S. Swaminathan, B. M. Craven, M. A. Spackman, and R. F. Stewart, Acta Crystallogr. B Struct Sci. 40, 398–404 (1984).
- 11. K. Dziubek, M. Citroni, S. Fanetti, A. B. Cairns, and R. Bini, J. Phys. Chem. C **121**, 2380–2387 (2017).
- 12. K. Roszak and A. Katrusiak, J. Phys. Chem. C 121, 778–784 (2017).
- 13. S. Anker, D. McKechnie, P. Mulheran, J. Sefcik, and K. Johnston, Cryst. Growth Des. 24, 143–158 (2024).
- 14. J. Wang, R. M. Wolf, J. W. Caldwell, P. A. Kollman, and D. A. Case, J. Comput. Chem. **25**, 1157–1174 (2004).
- 15. S. J. Weiner, P. A. Kollman, D. T. Nguyen, and D. A. Case, J. Comput. Chem. 7, 230–252 (1986).
- 16. W. L. Jorgensen, D. S. Maxwell, and J. Tirado-Rives, J. Am. Chem. Soc. **118**, 11225–11236 (1996).
- 17. D. Frenkel and J. P. McTague, Annu. Rev. Phys. Chem. 31, 491–521 (1980).
- 18. D. Frenkel and A. J. C. Ladd, J. Chem. Phys. 81, 3188-3193 (1984).
- 19. B. Kuchta and R. D. Etters, Phys. Rev. B 47, 14691 (1993).
- 20. J. L. Aragones, E. G. Noya, C. Valeriani, and C. Vega, J. Chem. Phys. 139, 034104 (2013).
- 21. M. Salvalaglio, C. Perego, F. Giberti, M. Mazzotti, and M. Parrinello, Proc. Natl. Acad. Sci. U.S.A. 112, E6–E14 (2015).
- 22. F. Giberti, M. Salvalaglio, M. Mazzotti, and M. Parrinello, Chem. Eng. Sci. **121**, 51–59 (2015).
- 23. T. Mandal and R. G. Larson, J. Chem. Phys. 2017 146, 134501 (2017).
- 24. C. Schoonen and J. F. Lutsko, Phys. Rev. Lett. **129**, 246101 (2022).
- 25. G. A. O'zpınar, W. Peukert, and T. Clark, J. Mol. Model. 16, 1427–1440 (2010).
- 26. C. D. Wick, J. M. Stubbs, N. Rai, and J. I. Siepmann, J. Phys. Chem. B **109**, 18974–18982 (2005).
- 27. H. Lorentz, A. Ann. Phys. 12, 127 (1881).
- 28. Berthelot, D. C. r. hebd. Se'anc. Acad. Sci. 126, 127 (1889).
- 29. J. Mullin, Crystallization, 4th ed. (Butterworth-Heinemann: Oxford, 2001). pp 478–535.
- 30. N. Sklar, M. E. Senko, and B. Post, Acta Crystallogr. 14, 716–720 (1961).

- 31. K. Suzuki, S.-i. Onishi, T. Koide, and S. Seki, Bull. Chem. Soc. Japan 29, 127–131 (1956).
- 32. D. Ferro, G. Barone, G. Della Gatta, and V. Piacente, J. Chem. Thermodyn. 19, 915–923 (1987).
- 33. V. N. Emel'yanenko, G. J. Kabo, and S. P. Verevkin, J. Chem. Eng. Data 51, 79-87 (2006).
- 34. D. Zaitsau, G. Kabo, A. Kozyro, and V. Sevruk, Thermochim. Acta **406**, 17–28 (2003).
- 35. H. De Wit, J. Van Miltenburg, and C. De Kruif, J. Chem. Thermodyn. 15, 651–663 (1983).
- 36. M. P. Allen and D. J. Tildesley, *Computer Simulation of Liquids* (Oxford University Press: Oxford, England, 1987).
- 37. J. I. Siepmann and D. Frenkel, Mol. Phys. **75**, 59 (1992).
- 38. F. A. Escobedo and J. J. de Pablo, J. Chem. Phys. 102, 2636–2652 (1995).
- 39. J. C. Shelley and G. N. Patey, J. Chem. Phys. 102, 7656–7663 (1995).
- 40. M. Vendruscolo, J. Chem. Phys. **106**, 2970–2976 (1997).
- 41. T. J. H. Vlugt, M. G. Martin, B. Smit, J. I. Siepmann, and R. Krishna, Mol. Phys. **94**, 727 (1998).
- 42. M. G. Martin and J. I. Siepmann, J. Phys. Chem. B 103, 4508 (1999).
- 43. C. D. Wick and J. I. Siepmann, Macromolecules 33, 7207–7218 (2000).
- 44. A. Sepehri, T. D. Loeffler, and B. Chen, J. Chem. Phys. 141, 074102 (2014).
- 45. A. Sepehri, T.D. Loeffler, and B. Chen, J. Chem. Theory Comput. 13, 1577 (2017).
- 46. A. Sepehri, T. D. Loeffler, and B. Chen, J. Chem. Theory Comput. 13, 4043 (2017).
- 47. M. N. Rosenbluth and A. W. Rosenbluth, J. Chem. Phys. 23, 356–359 (1955).
- 48. R. B. Nellas, M. E. McKenzie, and B. Chen, J. Phys. Chem. B 110, 18619–18628 (2006).
- 49. T. D. Loeffler, A. Sepehri, and B. Chen, J. Chem. Theory Comput. 11, 4023 (2015).
- 50. K. J. Oh and X. C. Zeng, J. Chem. Phys. 112, 294 (2000).
- 51. B. Chen, J. I. Siepmann, K. J. Oh, and M. L. Klein, J. Chem. Phys. 116, 4317 (2002).
- 52. G. M. Torrie and J. P. Valleau, J. Comput. Phys. **23**, 187–199 (1977).
- 53. R. Becker and W. Döring, Ann. Phys. **24**, 719 (1935).
- 54. M. Volmer and A. Weber, Z. Phys. Chem. 119, 277 (1926).
- 55. A. Laaksonen, V. Talanquer, and D. W. Oxtoby, Annu. ReV. Phys. Chem. 46, 489 (1995).
- 56. D. Kashchiev, Nucleation: Basic Theory with Applications (Butterworth-Heinemann, Oxford, 2000).

- 57. J. Merikanto, E. Zapadinsky, A. Lauri, and H. Vehkamäki, H., Phys. Rev. Lett. 98, 145702 (2007).
- 58. B. Chen, H. Kim, S. J. Keasler, and R. B. Nellas, J. Phys. Chem. B 112, 4067 (2008).
- 59. B. N. Hale, Metall. Trans. A 23, 1863 (1992).
- 60. B. N. Hale and D. J. DiMattio, J. Phys. Chem. B 108, 19780 (2004).
- 61. R. B. Nellas, S. J. Keasler, J. I. Siepmann, and B. Chen, J. Chem. Phys. 132, 164517 (2010).
- 62. T. D. Loeffler, D. E. Henderson, and B. Chen, J. Chem. Phys. 137, 194304 (2012).
- 63. T. D. Loeffler and B. Chen, J. Chem. Phys. 139, 234707 (2013).
- 64. P. J. Steinhardt, D. R. Nelson, and M. Ronchetti, Phys. Rev. B 28, 784 (1983).
- 65. P. R. ten Wolde, M. J. Ruiz-Montero, and D. Frenkel, J. Chem. Phys. 104, 9932 (1996).

Bond parameter		Angle parameter	
Bond	r [Å]	Angle	θ[°]
С-О	1.250	N-C-O	120.9
C-N	1.383	N-C-N	118.2
N-H	0.965	C-N-H / H-N-H	120.0
Nonbonding parameters			
Atom	σ [Å]	ε[Κ]	q [e]
С	3.72	34	0.884
O	3.05	79	-0.660
N	3.34	111	-0.888
Н	0	0	0.388

TABLE. 1. Both bonded and non-bonded parameters for the urea model used in this study.

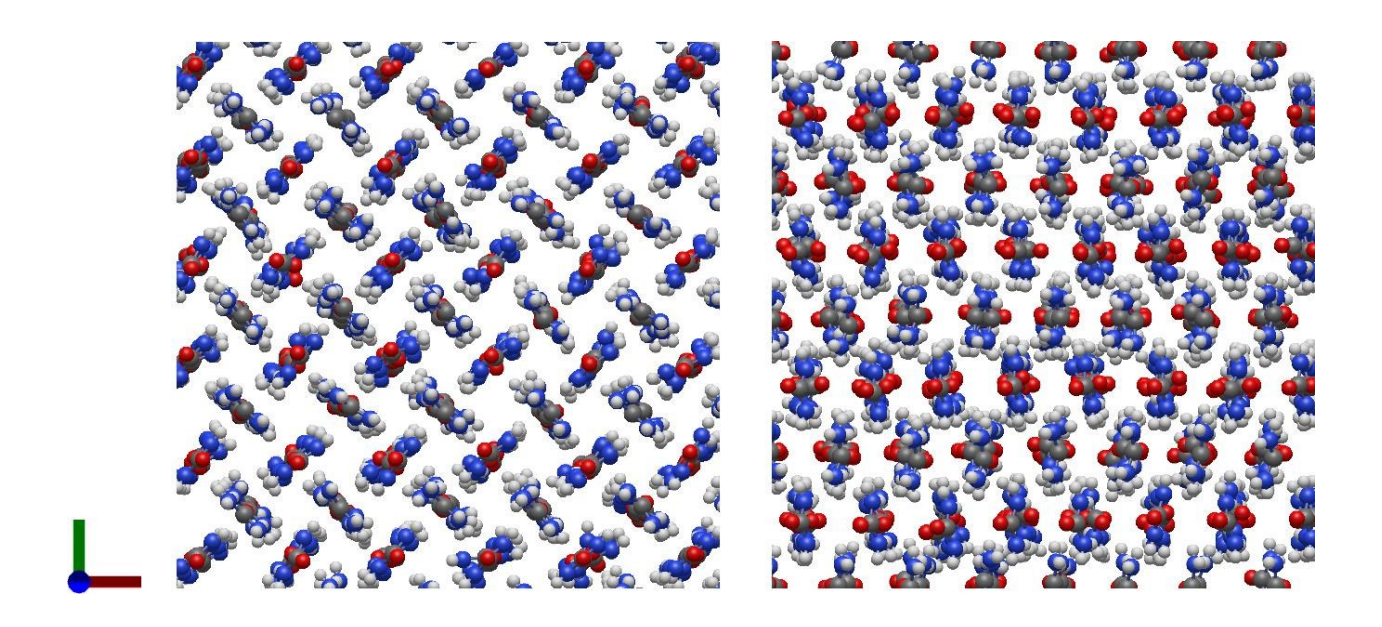


FIG. 1. Representative snapshots of form I (left) and form IV (right) from the bulk-phase simulation viewed from the *z*-direction. Color notations: carbon (grey), oxygen (red), nitrogen (blue), and hydrogen (white).

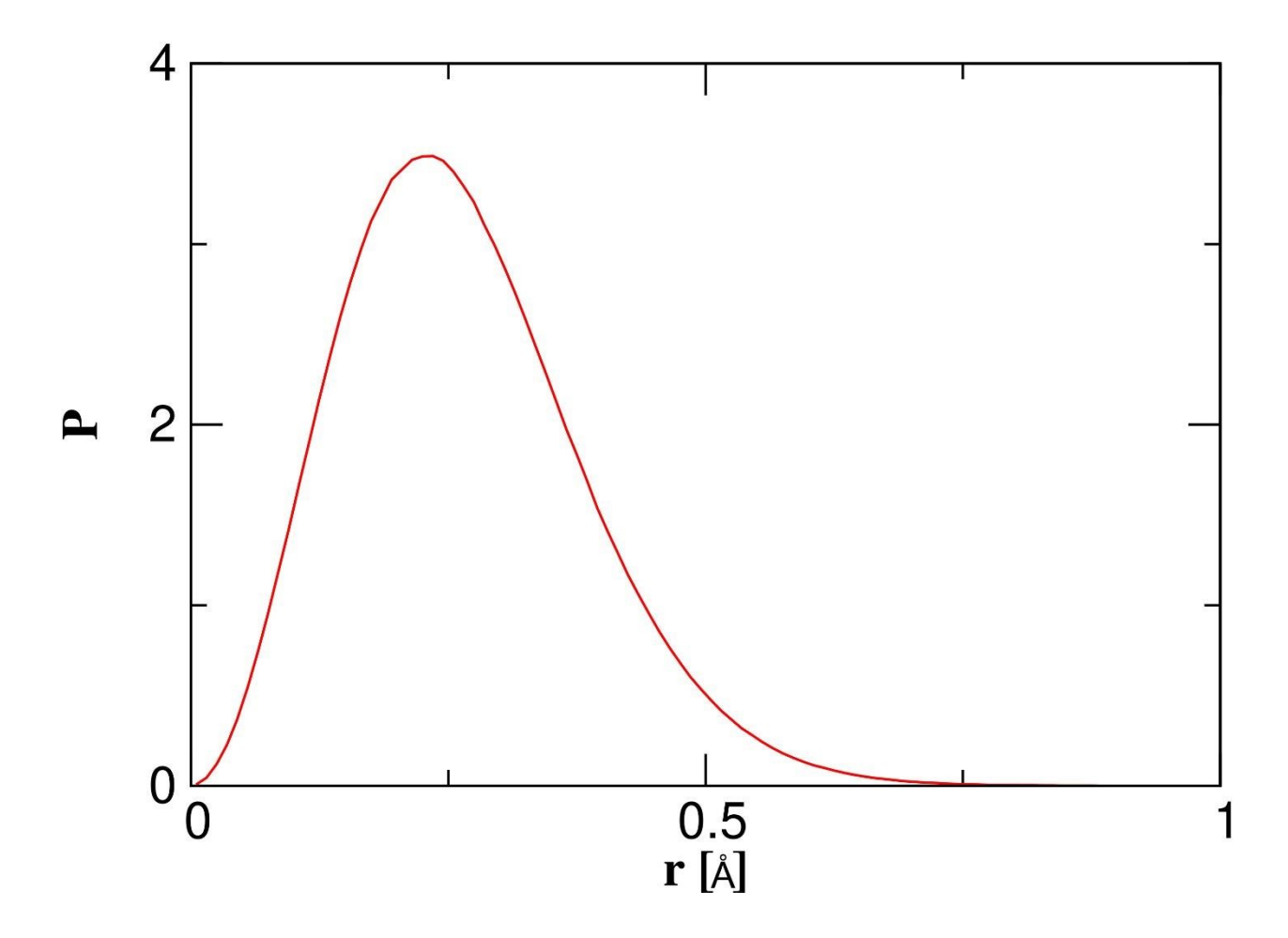


FIG. 2. Normalized probability of finding the carbon atom as a function of the distance from the lattice position.

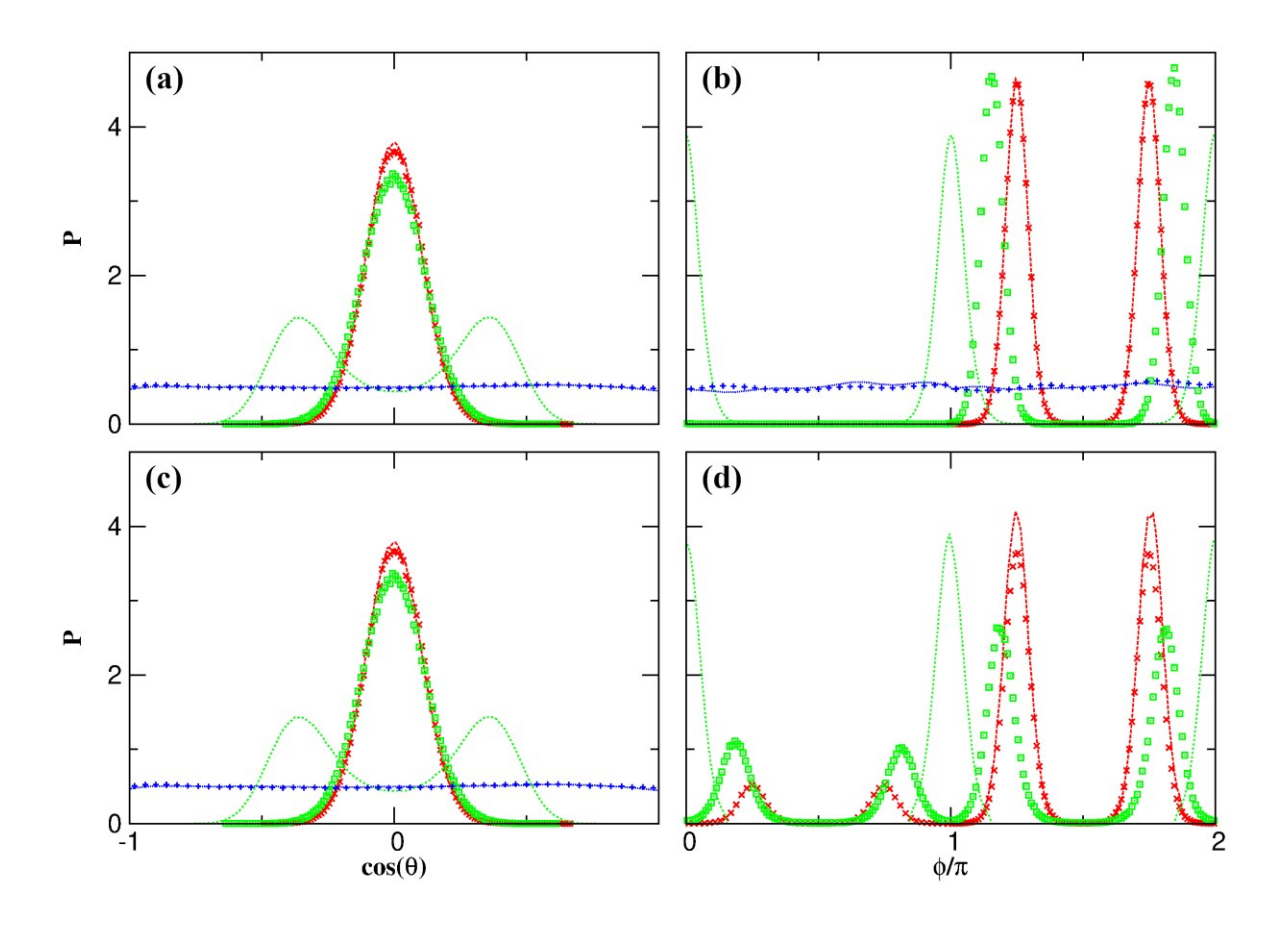


FIG. 3. Normalized distribution of the cosine of the angle θ between the normal vector of the molecular plane of the urea and the *z*-axis, and the ϕ angle between the projection of this vector onto the *xy*-plane and the *x*-axis. Shown in panels (a) and (b) are the results obtained for both bulk phases (lines) and clusters containing 800 particles (symbols) without the orientational constraint for form I (red), form IV (green), and liquid (blue). Shown in panels (c) and (d) are the results obtained for clusters containing 200 particles with (lines) or without (symbols) the orientational constraint for form I (red) and form IV (green). For clusters, the results are averaged over those particles if the carbon position is within 10 Å from the center of the cluster, defined by averaging the carbon positions of all particles.

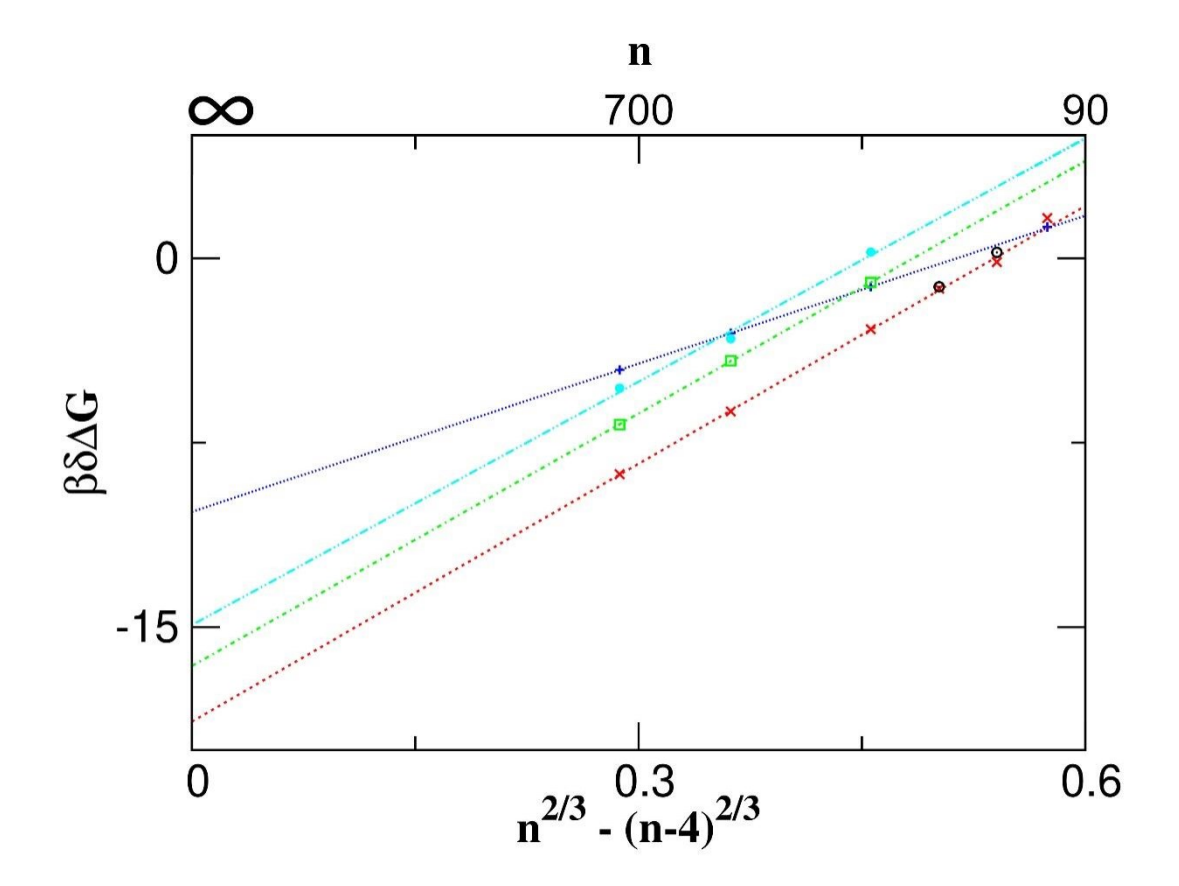


FIG. 4. $\delta\Delta G$ (= $\Delta G(n)$ – $\Delta G(n$ –4)) as function of $n^{2/3}$ – (n–4) $^{2/3}$ obtained at an ideal gas phase density of 4 × 10⁻¹¹ molecule/Å³ for form I (red), form IV with (green) or without (cyan) the ϕ constraint bcc (crosses), and liquid urea (blue). For form I, a few data points obtaining using the regular AVBMC are shown as black circles. Linear fits performed over the size range between 200 and 800 are also shown.

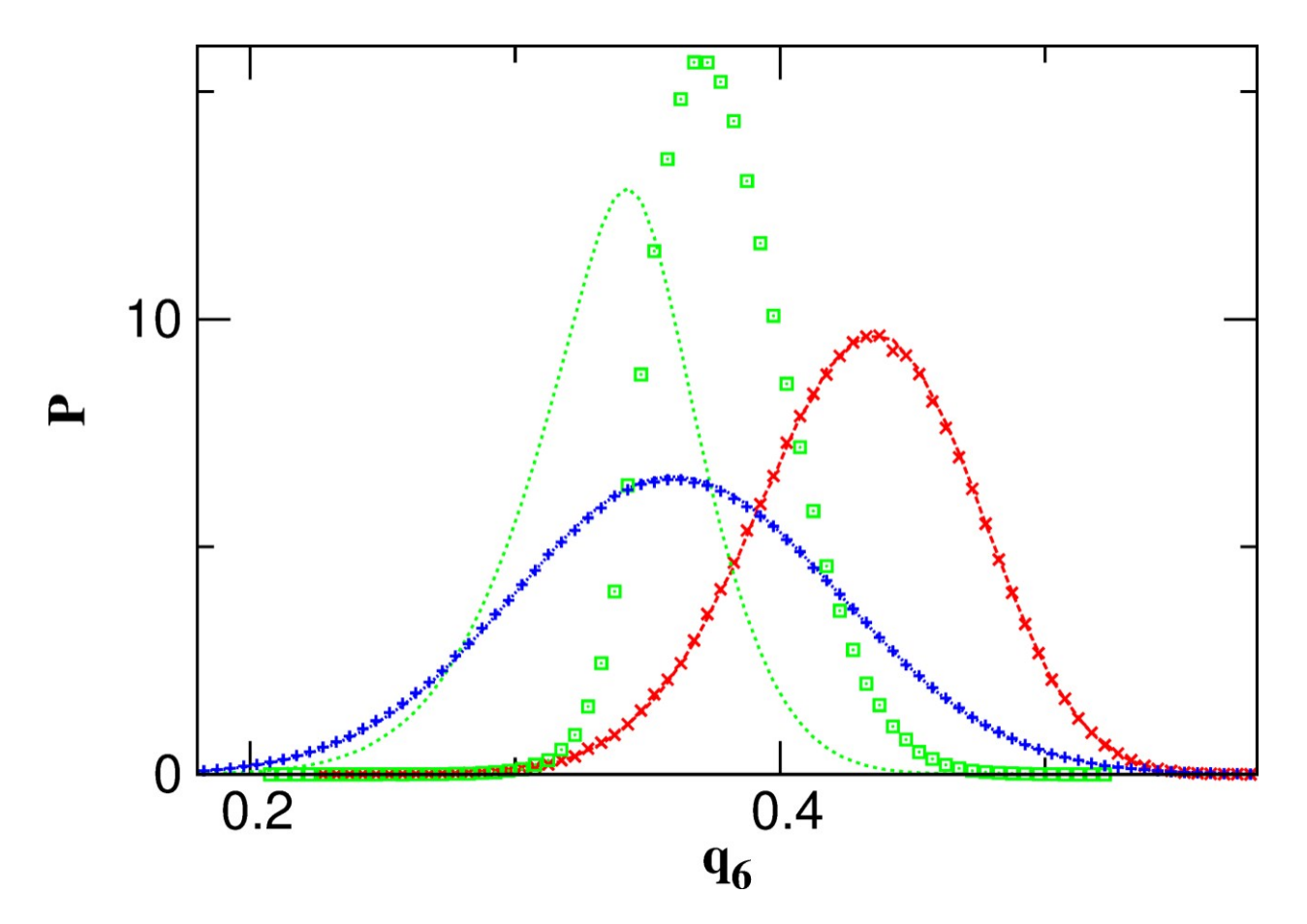


FIG. 5. Normalized distribution of the local order parameter q_6 . For bulk phases (shown as lines), the results are obtained by averaging over all particles. For clusters (shown as symbols) with 800 molecules sampled with the original LB-AVBMC, the results are averaged over those particles if the carbon position is within 10 Å from the center of the cluster, defined by averaging the carbon positions of all particles. The results are shown as red, green, and blue for form I, form IV, and liquid, respectively. For solid, the neighbors arranged in the eight corners of the unit cell are used for this analysis while for liquid, neighbors are defined when the distance between carbon atoms is within 6 Å.